PROGRESS REPORT ON HYDROGEN MASER DEVELOPMENT AT LAVAL UNIVERSITY

Jacques Vanier, Guy Racine, Ryszard Kunski and Marcel Picard

Laboratoire d'Electronique Quantique
Département de Génie Electrique
Université Laval
Québec G1K 7P4
Canada

ABSTRACT

The paper describes the physical construction of two hydrogen masers which have been under development at Laval University for a few years. Results of measurements made on one of the two masers are given. These include: cavity Q, thermal time constant, line Q, signal power output, magnetic shielding factor.

INTRODUCTION

In the hydrogen maser [1,2], the wall shift remains one of the major perturbations [3]. In the determination of the size of that perturbation one is faced with the problem of cavity tuning accuracy. In the standard or classical technique of tuning by means of spin-exchange broadening [4], one requires, first, a good medium term stability in the range of averaging times from 10 seconds to 1 000 seconds. Secondly, one requires the possibility of changing the line quality factor, Q_ℓ, by a large amount. Those two requirements are much more stringent if the final aim is a measurement of the stability of the wall shift with time. There are reasons to believe that such an effect may exist, and reports on the long term stability of the wall shift, for a given maser design, have been given [5]. That effect, if common to all masers, would have important consequences when the maser is used in precision time and time interval applications. Our intent is to measure accurately the wall shift over long periods of time and to determine its actual stability. For that reason we have started the development of two new hydrogen masers which 1) should have the required stability over the averaging times needed and 2) should be tunable easily by means of the spin exchange interaction.

The present paper is a progress report on this development. It describes briefly: a) the main features of the physical construction of the masers, b) the electronic control systems, c) the phase-locked-loop system for locking a 100 MHz crystal oscillator to the maser signal. The paper gives also results of measurements of the actual characteristics of one of the two masers.

THE MASERS PHYSICAL CONSTRUCTION

A schematic drawing of the masers is given in Figure 1. A photograph of an actual maser is shown in Figure 2. The design follows from logical conclusions derived from a study of the various types of masers made by other researchers working in that field, and from an analysis of the results published. An intercomparison of the performance of several of the best masers fabricated up to now has been reported earlier [6]. From the results published, it is concluded that the main limiting factors of the frequency stability of the hydrogen maser are in general:

1) sensitivity to temperature fluctuations in the environment,
2) sensitivity to barometric pressure fluctuations,
3) sensitivity to external magnetic field fluctuations.

The masers were thus designed in such a way as to try to minimize their sensitivity to those perturbations.

1) It is believed that the main cause of instability of a temperature-compensated-cavity is due to temperature gradients in the cavity structure itself. A perfectly compensated cavity by definition will have a zero temperature coefficient. However, the temperature compensation usually done at one end of the cavity coupled to the temperature sensitive dielectric constant of the storage bulb makes the cavity rather unsymmetrical. As a consequence gradients play a very important role. The present design tries to avoid these gradients by means of two heavy *"thermal barriers"* made of aluminum and placed inside a heavy vacuum enclosure. These barriers are held together by means of ceramic insulators for rigidity. The cavity itself is made of quartz. It is thermally compensated by means of a re-entrant OFHC copper disk attached with three OFHC copper rods to one of the quartz end plates. The quartz cavity cylinder and bottom plate are coated with pure silver, by chemical deposition. The loaded quality factor is 35 000 with a coupling coefficient $\beta = 0.2$. The cavity is held inside the inner thermal barrier by means of Be-Cu springs. Furthermore the whole assembly is held at constant temperature by means of 10 independent temperature regulators placed symmetrically around the structure. Such a structure has a very long time constant. Figure 3 is a preliminary result showing the variation of the cavity resonance frequency as a function of time after a step function of temperature has been applied to the vacuum enclosure. The long settling time is essentially a measure of the decoupling between the cavity and the outside world. The temperature coefficient in that case is of the order of 200 HZ/°C. If the cavity can be held to $\pm .001$ °C we expect a frequency stability of $\pm 2 \times 10^{-15}$.

2) That same structure design has also the advantage of decoupling the cavity from external barometric pressure fluctuations. In practice it is observed, that the barometric pressure affects the resonance frequency of the cavity through a mechanical distortion. The importance

of this distortion is a function of the nature of the bottom plate of the vacuum envelope and of the type of attachment of the cavity to that bottom plate. In the present design, the mechanical decoupling created by the thermal shields and the spring mounting of the cavity should make this effect negligible. Conclusions on the performance of the design will be drawn from actual measurements.

3) The sensitivity to magnetic field is expressed through the following equation:

$$\nu = \nu_o + 2752 < B^2 >$$

Normally the maser operates in an induction of 1 mgauss. The sensitivity to magnetic field fluctuations is then given by the expression:

$$\delta\nu_B = 5.5\ \Delta B$$

In order to achieve frequency fluctuations less than 1×10^{-15}, one requires that the magnetic fluctuations be less than 0.25 μgauss. We have chosen a magnetic shielding system consisting of 5 moly-permalloy cylindrical enclosures with end caps [7]. The bottom caps have a 2 inch hole for the pumping duct. The dimensions of these shields are respectively:

Shield N°	1	2	3	4	5
Radius R (inch)	12	11	10	9	8
Length L (inch)	30	28	26	24	22
Thickness (inch)	0.050	0.025	0.025	0.025	0.025

Table 1 - Dimensions of the magnetic shields

The shielding factor is defined as follows:

$$S = \frac{\text{External field}}{\text{Internal field}} = \frac{H_{ext}}{H_{int}} = \text{Shielding factor}$$

or

$$S_{dB} = 20 \log \frac{H_{ext}}{H_{int}}$$

For a single cylindrical shield with end caps, the shielding factors are given by the expressions [8]:

$$S_t = \frac{1}{2}\ \mu\ t'$$

$$S_\ell = 2\ D\ \mu\ t' \left[1 + \frac{R}{L}\right]^{-1}$$

where subscript t refers to transverse while subscript ℓ refers to longitudinal. In these expressions t' is the ratio of the material thickness to the shield radius R, L is the length of the shield, μ

is the permeability of the material at the actual level of magnetic induction B_m inside the material. The value of B_m is obtained from the relation:

$$B_m = 2 \gamma H_{ext}/t'$$

where γ is a geometrical factor close to 1. The symbol D stands for demagnetisation factor. In our case it has a value between 0.26 and 0.28 for the 5 shields considered. The calculated values of S_t and S_ℓ for the five shields are given in Table 2. The measured values of S_t are also given.

$S_i(H_{ext})$ \ Shield N°	1	2	3	4	5
S_ℓ (1 oersted) calculated	165	145	145	145	148
S_t (1 oersted) calculated	181	147	150	153	164
S_t (1 oersted) measured	125	118	140	130	125
S_ℓ (Low field limit) calculated	50	27	30	33	35
S_t (Low field limit) calculated	62	34	38	42	47

Table 2 - Calculated and measured shielding factor of the five individual shields

The measured values are slightly lower than the calculated ones. This may be due to the fact that the actual μ of the material used varies slightly from shield to shield and does not have exactly the tabulated value.

In the case of two concentric shields with end caps the transverse shielding factor is given by:

$$S_t = S_{t_1} \times S_{t_i} \left(1 - \frac{R_i^2}{R_1^2}\right) + S_{t_1} + S_{t_i}$$

where i refers to the inner shield and 1 refers to the outer shield. The value of S_{t_i} has to be taken as the low field value. We have made measurements with the four smaller shields placed one at a time inside shield #1. The results for the transverse shielding factor are given in Table 3. This table gives also the calculated values for the combinations in question, using the calculated values shown in Table 2. These results are also shown in Figure 4. The agreement between the calculated and the measured values is relatively good. Finally, the shielding factors S_t and S_ℓ were measured for the cumulative effect of the five shields. The results are shown in Figure 5 and illustrate

Shields Combination	N° 1 + 2	N° 1 + 3	N° 1 + 4	N° 1 + 5
S_t calculated [dB]	61.6	67.2	71.0	73.9
S_t measured [dB]	61.1	67.7	70.5	72.0

Table 3 - Calculated and measured values of the transverse shielding factor for various combinations of two shields.

the increase in shielding factor with the number of shields used. The maximum shielding factor of the five shields is thus:

S_t (1 oersted) = 128 dB ; measured
S_ℓ (1 oersted) = 100 dB ; measured

The longitudinal shielding factor is lower then the transverse shielding factor as expected. The value obtained means that external longitudinal fluctuations are attenuated by a factor of 10^5. This also means that, for a frequency stability better than 10^{-15}, a fluctuation of the external field larger than 25 mgauss cannot be tolerated. Although the measurements reported here were done in a field 1 gauss, they are expected to apply approximately in the earth's field. This is due to the fact that only the outside shield changes its state of magnetization and that it is not saturated. Consequently, the overall shielding factor is not much affected. We expect that, with the present arrangement, we can tolerate a fluctuation of the earth's field of 10%, and still meet the requirement on stability set above.

Two other important items in the hydrogen maser construction are the source and the storage bulb.

1) In the hydrogen source, we have paid attention specially to the plasma-glass interaction. To minimize this effect we have used a large glass envelope as the dissociator. It is essentially a glass cylinder 2 inches long and two inches in diameter. The plasma is excited by a transistorized oscillator (100 MHz, 3 watts) whose tank circuit surrounds the discharge bulb.

The hydrogen pressure is stabilized with the help of a servo system controlling the temperature of a "Ag - Pd" hydrogen leak. The temperature is measured with a thermistor bead. The hydrogen leak is made of a fine finger glove, 4 cm long, 1 mm in diameter, and 0.1 mm thick [9]. The heating current passes directly through the finger glove. Approximately 1.5 A is required in normal operation. The source is completely assembled with Cajon fittings and copper gaskets. A block diagram of the system is shown in Figure 6. The dynamic response of the whole servo was tested with a step function command. The results are shown in Figure 7. It is observed that the time for equilibrium to be

achieved is about 5 seconds. This fast response is extremely important in regards to cavity tuning by means of spin exchange broadening.

2) The storage bulb: the storage bulb of the maser is made of quartz. In one of the masers it is a sphere 15 cm in diameter and coated with FEP 120 Teflon. The bulb collimator is made of 12 small tubings of commercial Teflon clustered at the entrance of the bulb. That approach has the advantage of presenting a large opening to the incoming beam, while holding the bulb escape time constant long. The arrangement works extremely well in the sense that the bulb line Q is very high and the maser oscillates at very low hydrogen fluxes. A typical result is shown in Figure 8. In that figure the signal output in arbitrary units and the line Q are plotted as a function of the pressure read on the servo control. In Figure 9, the inverse of the line Q is plotted as a function of pressure. This graph permits an extrapolation to zero pressure and gives the value of the line Q without spin exchange interaction. In the present case it is observed that the low pressure limit line Q is 3.2×10^9 while the high pressure limit is 9.6×10^8. This corresponds to a variation greater than 10 in flux between the low pressure and the high pressure flux thresholds. The quality factor q of the maser is evaluated to be approximately 0.10. This is calculated from the theory developed in Reference [2].

The accuracy to which the maser can be tuned is given by [10]:

$$\frac{\delta_{offset}\ (LP)}{\nu_o} = \frac{\left(\nu_m\ (LP) - \nu_m\ (HP)\right)}{\nu_o}\left[1 - \frac{Q_\ell\ (LP)}{Q_\ell\ (HP)}\right]^{-1}$$

where $\left(\nu_m\ (LP) - \nu_m\ (HP)\right)$ is the difference in frequency of the maser between low and high pressure of hydrogen in the storage bulb and, $Q_\ell\ (LP)$ and $Q_\ell\ (HP)$ are the low pressure and high pressure line Q's possible. The accuracy to which $\left(\nu_m\ (LP) - \nu_m\ (HP)\right)$ can be measured can be taken as the stability of the masers over the time of measurements. If a stability of 2×10^{-15} is achieved we thus have, from the line Q measurements reported here, a calculated tuning accuracy of about 4×10^{-15}.

ELECTRONIC CONTROLS

The following electronic systems are integral parts of the masers: 1) Power supplies, 2) VacIon control, 3) Hydrogen pressure control, 4) Magnetic field control, 5) Low frequency oscillator for the measurement of transitions between the Zeeman levels and subsequently for the determination of the magnetic induction at the site of the storage bulb, 6) Varactor control, 7) 100 MHz power oscillator to excite the hydrogen plasma in the dissociator, 8) Temperature regulators.

The design of these various controls has been made along the lines of established technology and published data in this field [11,12,13,14].

Their detailed description will be given somewhere else. It is necessary here only to mention that great care was taken in their construction in order to produce stable units. For example the temperature regulators are themselves regulated in temperature. The varactor control uses a Kelvin-Varley divider. The power sources are regulated at their input to each unit. We expect by means of these techniques to minimize external perturbations on the controls and unwanted perturbations on the maser frequency itself.

THE RECEIVER AND PHASE-LOCKED-LOOP

A receiver has been designed to detect the maser signal at 1.4 GHz and to phase-lock a basic quartz crystal oscillator to that signal. The frequency of the oscillator has been chosen as 100 MHz for reason of good phase stability at low cost. The design of that receiver is shown in Figure 10. It has been mounted as a breadboard and tests on its dynamic behaviour are being made. A final report will be given later.

CONCLUSION

In this paper we have described the construction of two hydrogen masers and have given experimental results on the operation of one of them. From the preliminary results obtained it is expected that the frequency stability will still be mainly affected by the thermal stability of the cavity. The magnetic field and the barometric pressure fluctuations should not affect the maser at the stability level above a few parts in 10^{15} which is our goal for averaging times of several hours.

ACKNOWLEDGEMENTS

We would like to thank MM. Roger Blier and Yvon Chalifour for their competent technical assistance. We would also like to thank Mr. Julien Morasse who has contributed greatly through his competence in the mechanical design of the masers. This program of research is sponsored by the National Sciences and Engineering Research Council of Canada and the Ministère de l'Education de la Province de Québec.

REFERENCES

[1] Kleppner, D., Goldenberg, H.M. and Ramsey, N.F., Phys. Rev. 126, 603-15, 1962.

[2] Kleppner, D., Berg, H.C., Crampton, S.B., Ramsey, N.F., Vessot, R.F.C., Peters, H.E., and Vanier, J., J. Phys. Rev. A. 138, 972-83, 1965.

[3] Vanier, J. and Larouche, R., Metrologia 14, 31-37, 1978.

[4] Vanier, J. and Vessot, R.F.C., App. Phys. Letters 4, 122-23, 1964.

[5] Morris, D., IEEE Trans. on Instr. and Meas., 339-342, 1978.

[6] Kuhnle, P.F., Proc. of the 11th PTTI Applications and Planning Meeting, 197-213, 1979.

[7] Allegheny, Ludlum, Brachenridge Penn.

[8] Gubser, D.E., Wolf, S.A., Cox, J.E., Rev. Sci. Instr. 50, 751-756, 1979.

[9] Viennet, J., Petit, P., Audoin, C., J. of Phys. E. Scientific Inst. 6, 257-261, 1973.

[10] Petit, P., Viennet, J., Barillet, R., Desaintfuscien, M., Audoin, C., Metrologia 10, 61, 1964.

[11] Vessot, R.F.C., Levine, M., Final Report Contract J.P.L. 9548118 Grant NSG 8052, 1977.

[12] Petit, P., Viennet, J., Barillet, R., Desaintfuscien, M., Audoin, C., Metrologia 10, 61, 1974.

[13] Reinhardt, V.S., Rueger, L.J., Space Electronics Systems Group, Report S3 LJR 002, September 1979.

[14] Beverini, N. and Vanier, J., IEEE Trans. on Instr. and Meas., IM-28, 100-104, 1979.

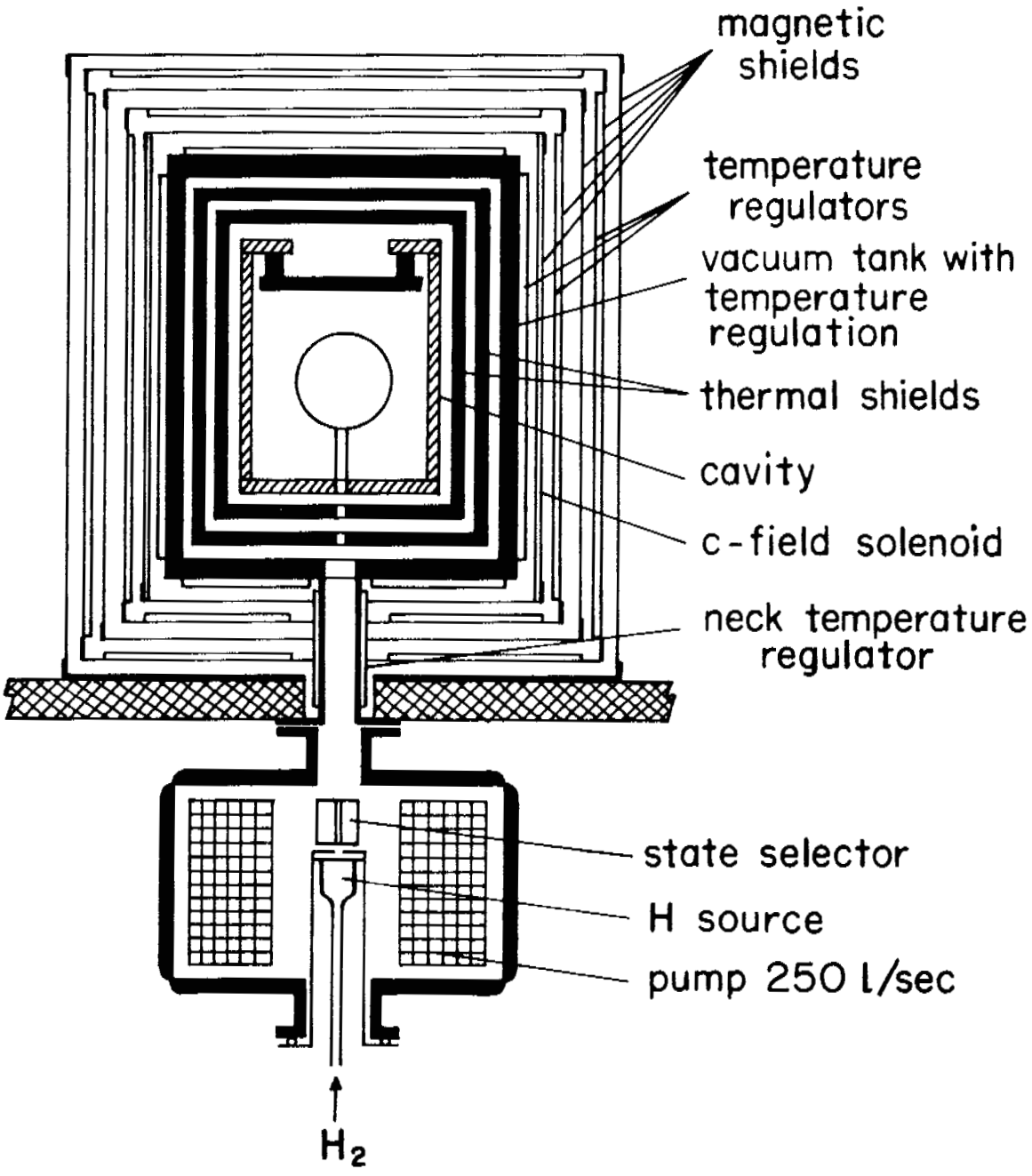

Figure 1 : Schematic drawing giving the main concepts used in the maser design.

Figure 2 : Photograph of one of the masers.

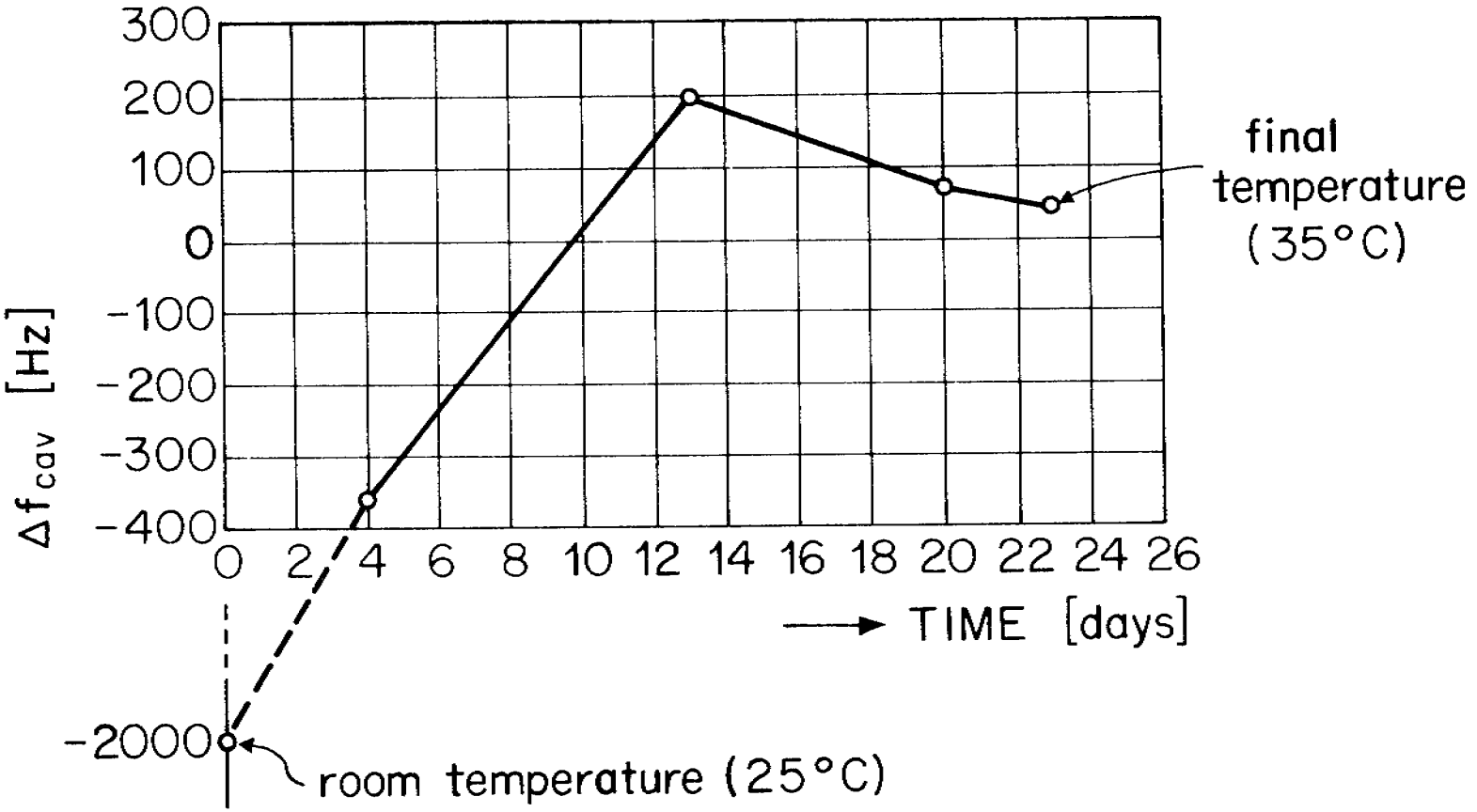

Figure 3 : Variation of the cavity resonance frequency after a step function variation of the temperature has been applied to the vacuum enclosure.

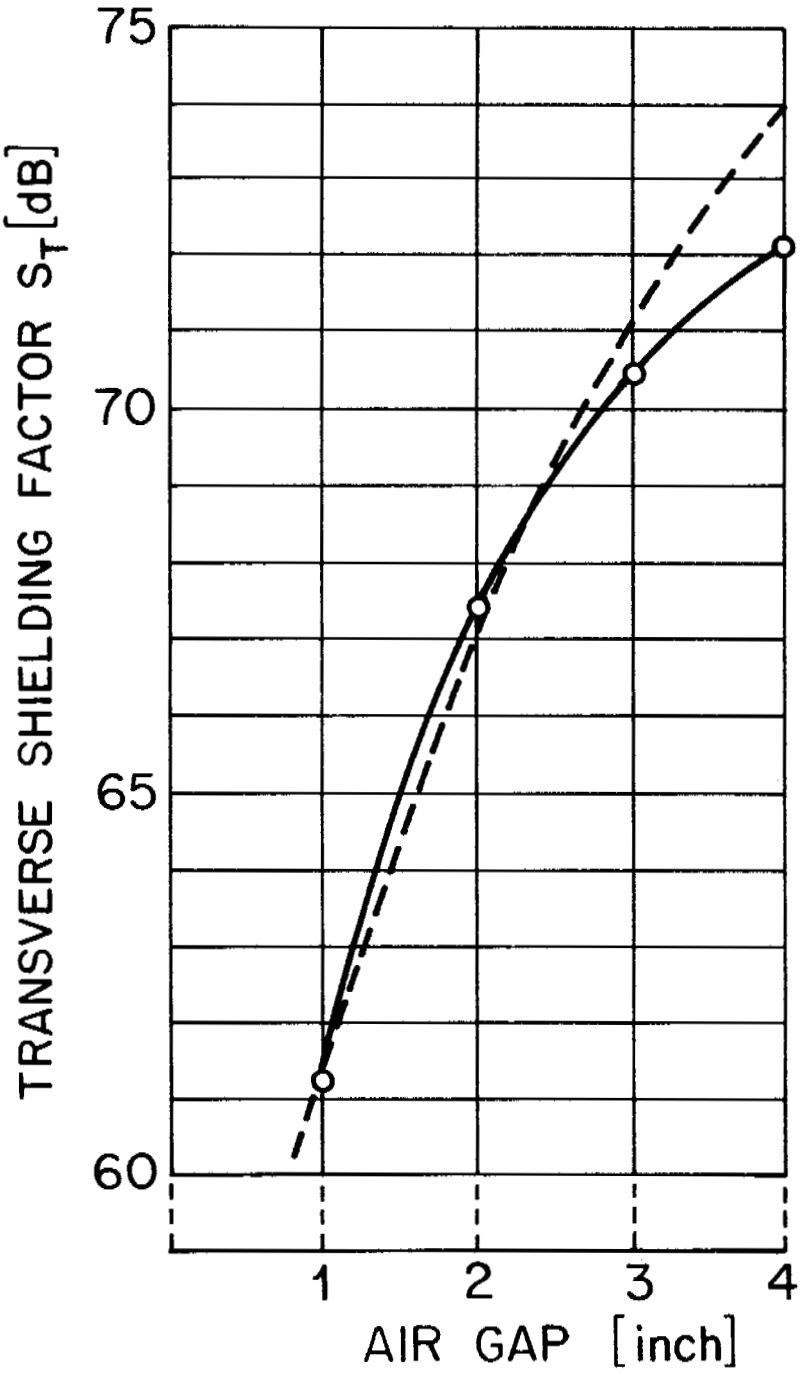

Figure 4 : Shielding factor as a function of the air gap ($B_{ext}=10^{-4}$T); solid line: experimental; dotted line: theoritical.

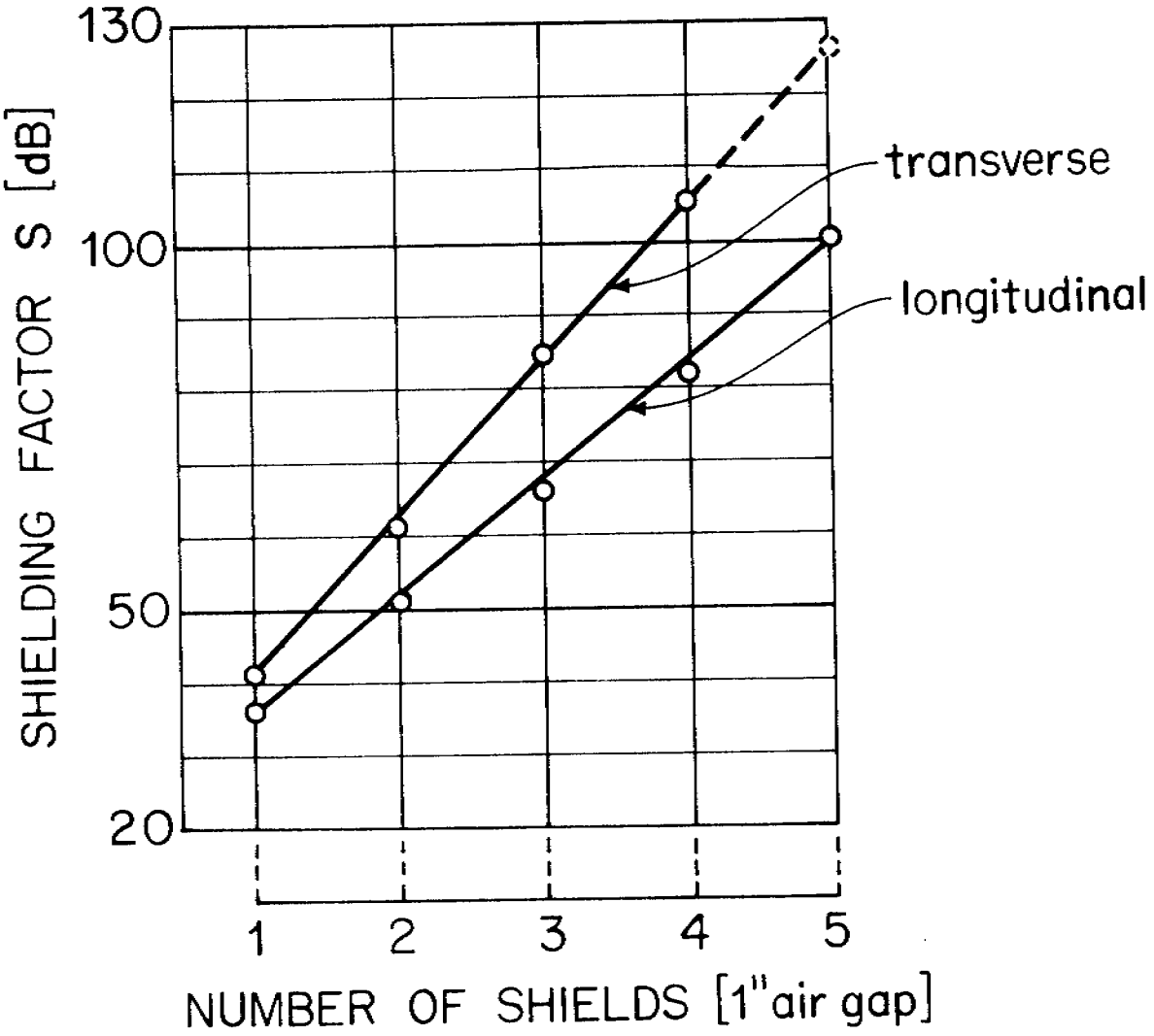

Figure 5 : Graph showing the increase in shielding factor with the number of concentric shields used.

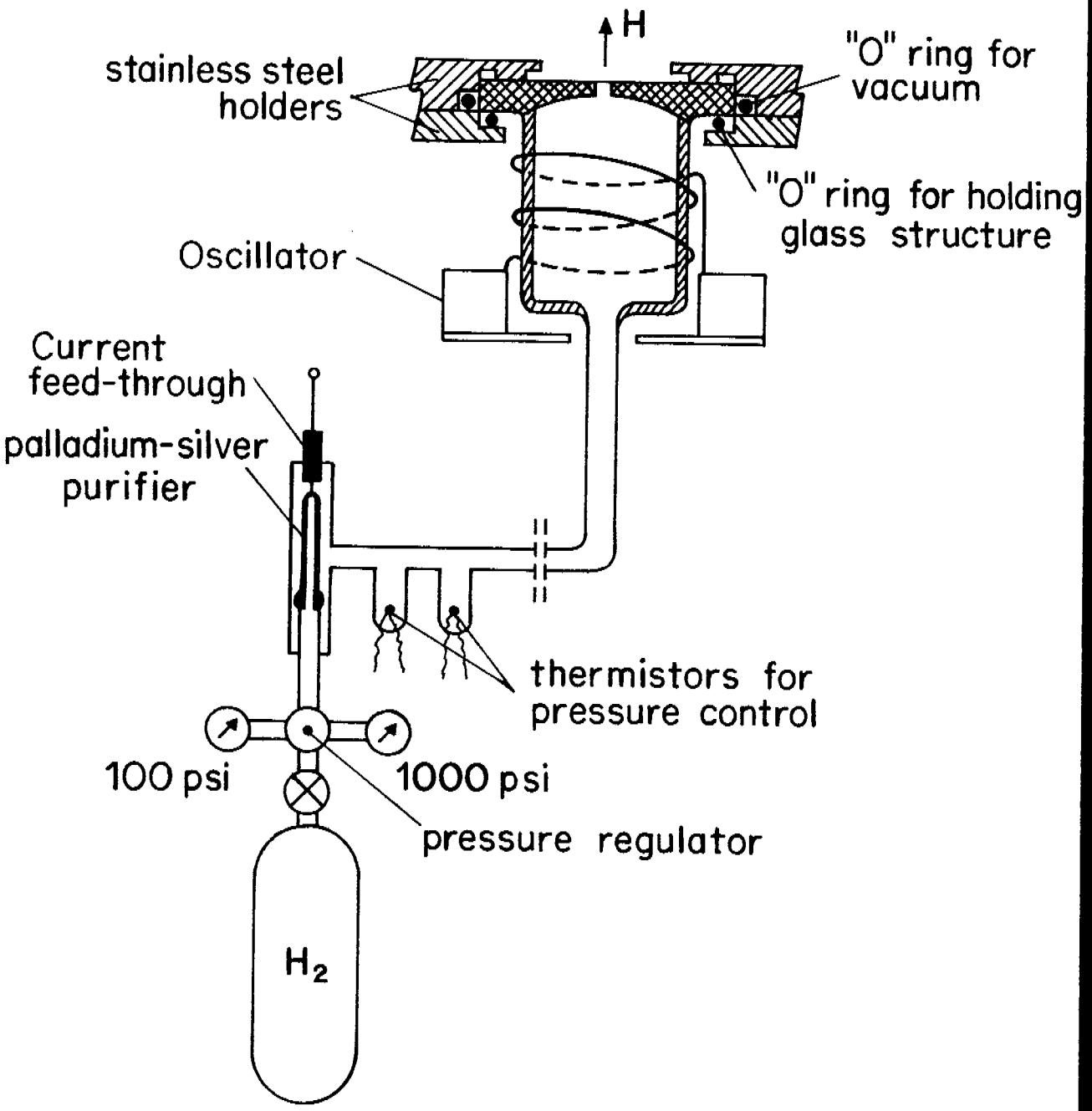

Figure 6 : Block diagram of the hydrogen source and the pressure control.

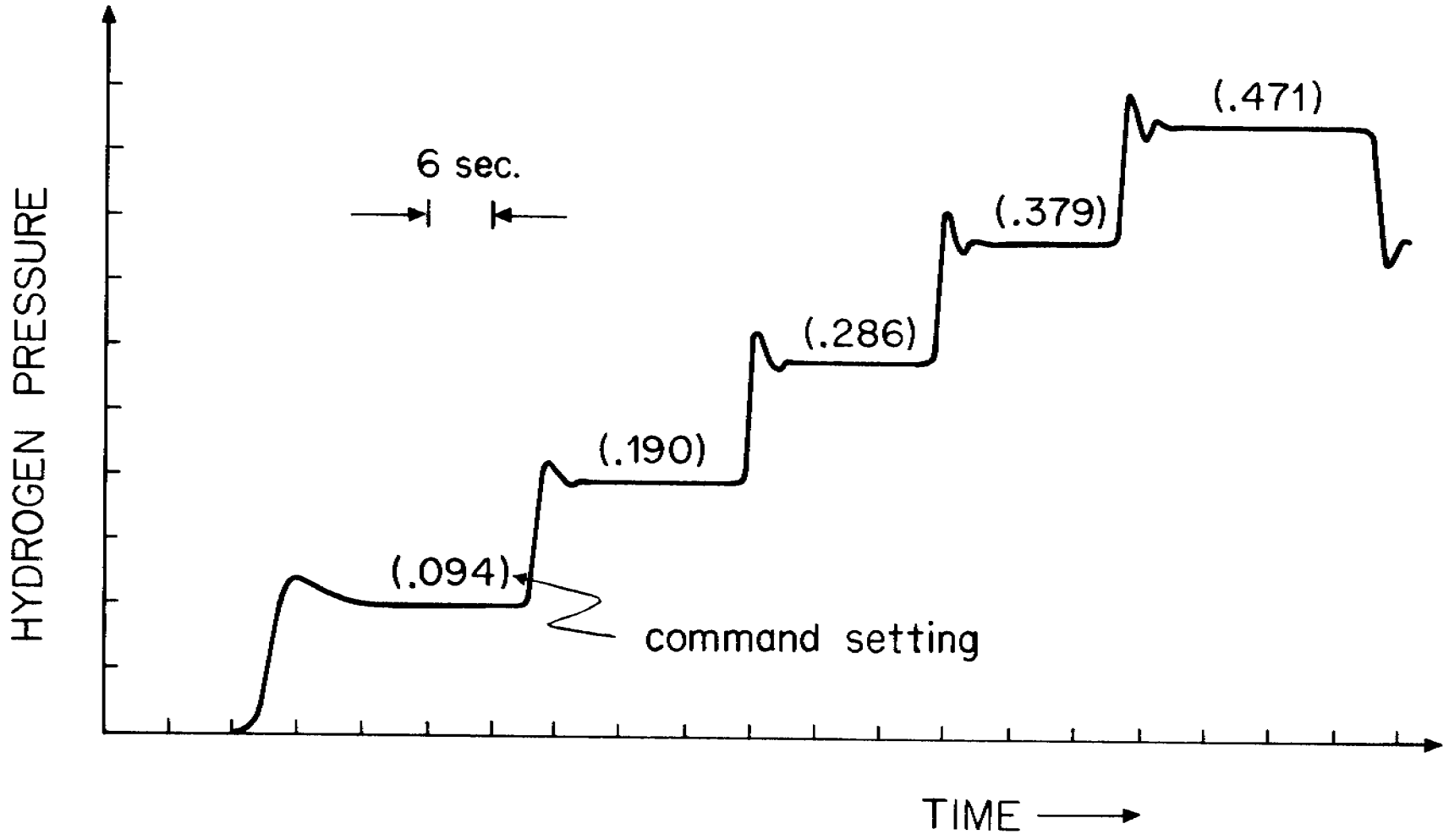

Figure 7 : Response of the pressure control system to a step function command.

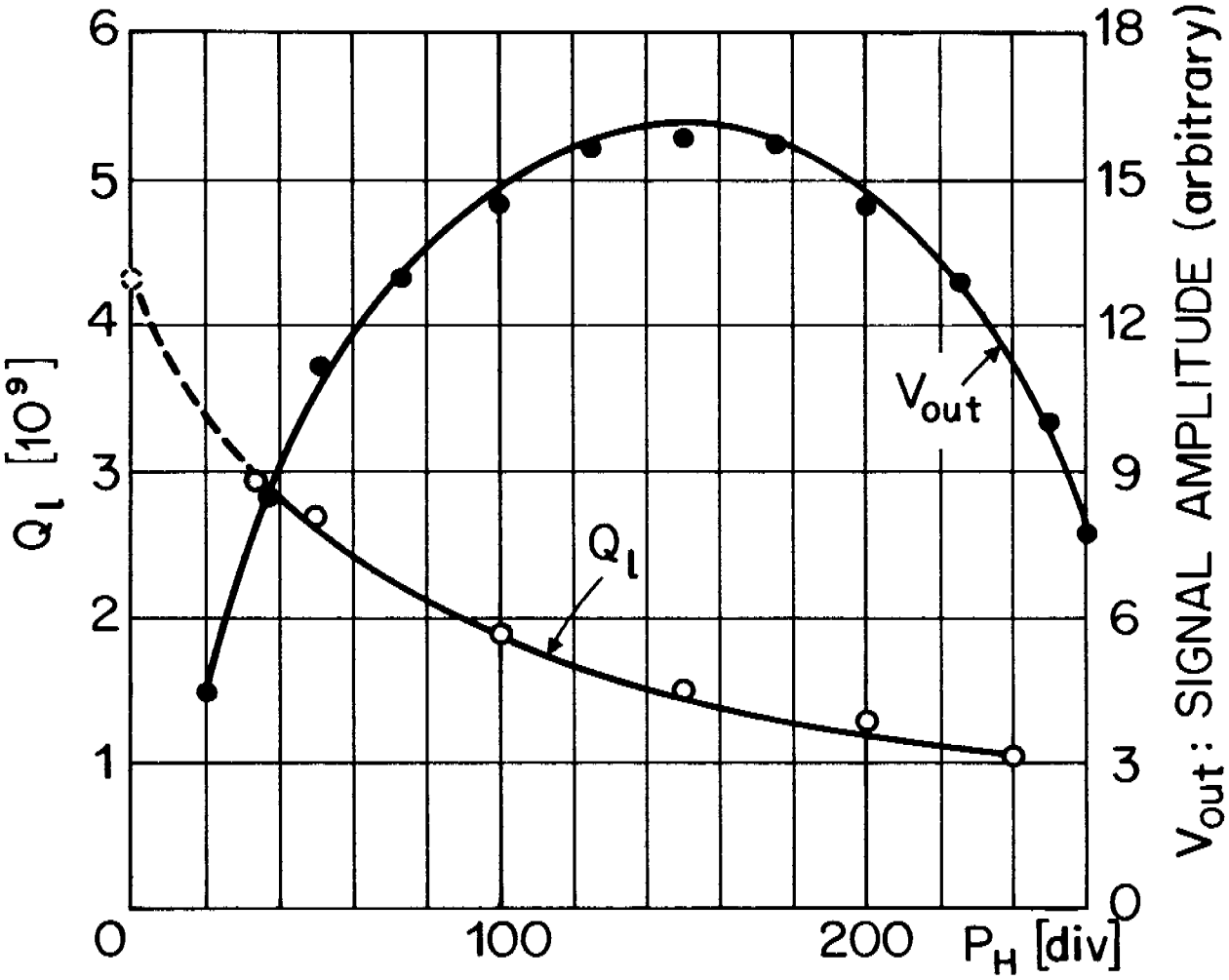

Figure 8 : Signal output of the maser and atomic line Q as a function of hydrogen pressure.

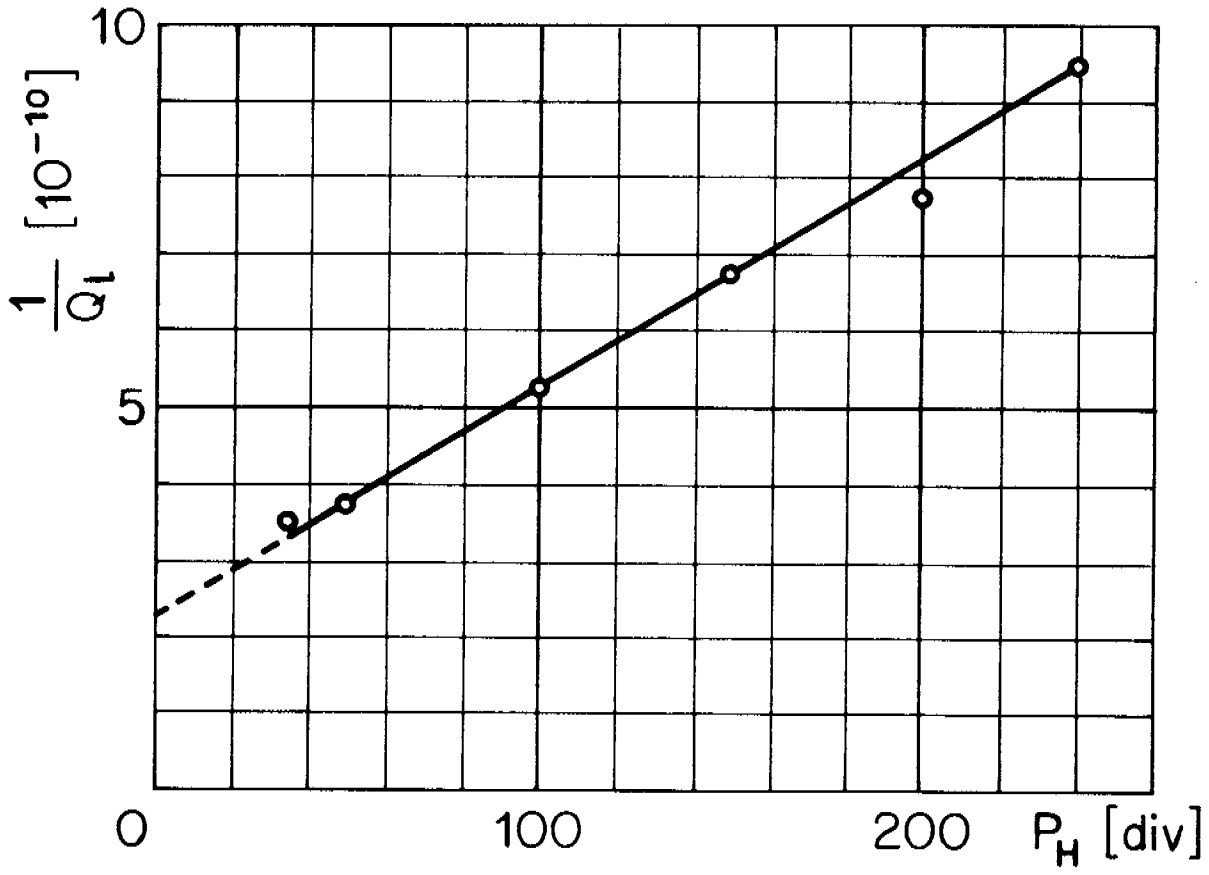

Figure 9 : Inverse of the line Q as a function of hydrogen pressure.

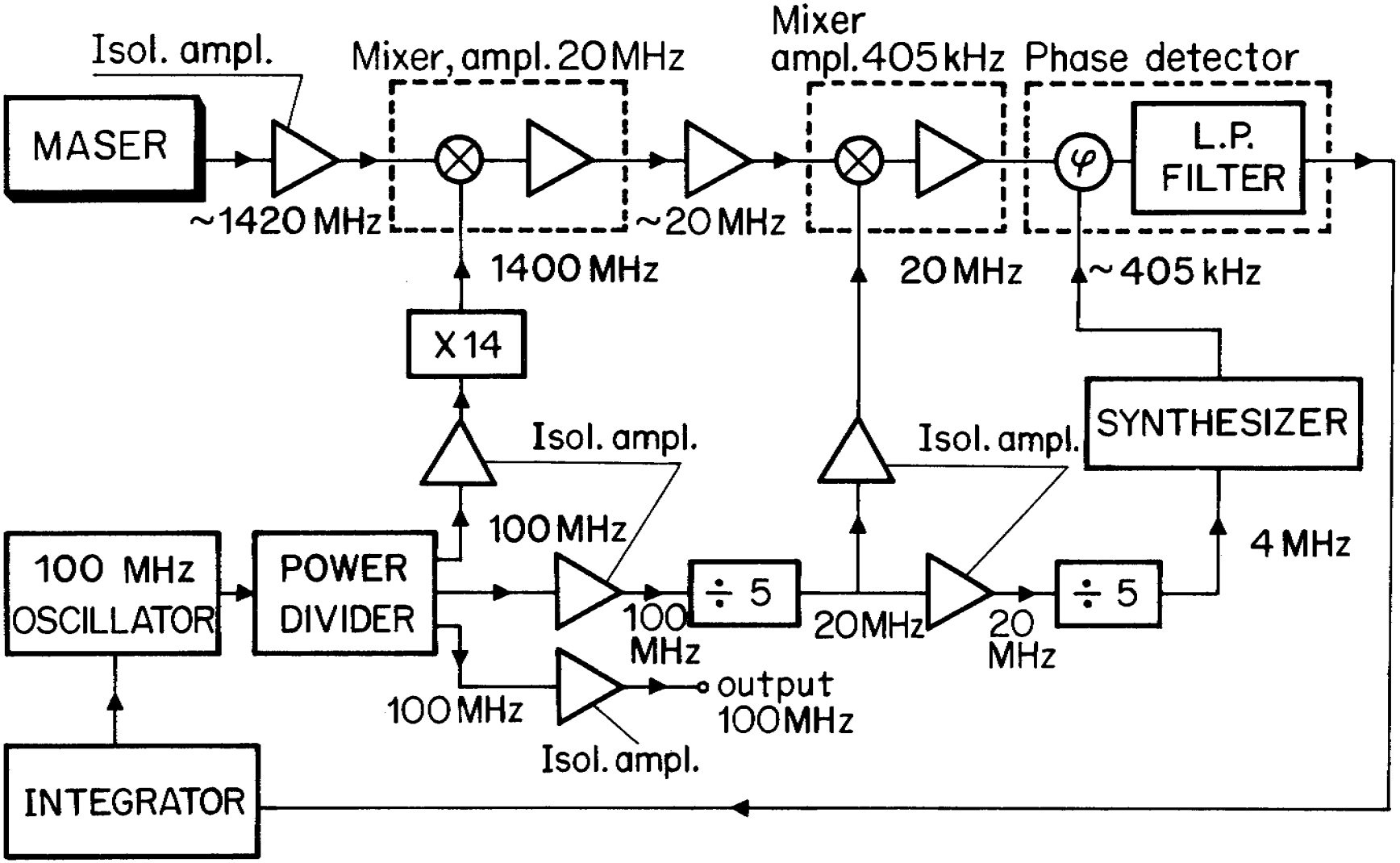

Figure 10 : Block diagram of the 100 MHz phase-locked-loop system for the hydrogen maser.

QUESTIONS AND ANSWERS

MR. DAVID HOWE, National Bureau of Standards

It was a very interesting experiment that you have set-up, Dr. Vanier, but I have a couple of questions with regard to the human factor with five shields. Was that a calculation or was that experimental?

DR. VANIER:

Oh, experimental.

MR. HOWE:

Okay, and what guarantee do you have that there are no residuals after degaussing? For example, creep will change that frequency, long-term --

DR. VANIER:

It does not, I have no guarantee of that.

MR. HOWE:

What kind of sensor are you using to determine the temperature? What accuracy is that sensor over long-term?

DR. VANIER:

The sensor, itself?

MR. HOWE:

Yes.

DR. VANIER:

For the magnetic field?

MR. HOWE:

No, I am sorry, for the temperature?

DR. VANIER:

It is standard; I can give you the company.

MR. HOWE:

And, was that an all glass thing?

DR. VANIER:

Yes. This was not really a problem here. When we say we want stability over let's say 1,000 seconds. We don't want stability over a year, we want to tune the maser all the time.

MR. HOWE:

I understand that, but maybe I don't understand. So, what you are saying is that you use the pressure method of tuning.

DR. VANIER:

We use the spin exchange broadening method of tuning, you have to. You could not rely on any temperature stability of the order of magnitude required here.

MR. HOWE:

I agree.

DR. VANIER:

To measure the wall shift on a long-term basis.

MR. HOWE:

Fine, that was a misunderstanding on my part.

And, last; at what level does the spin exchange come in with this method of tuning? In other words, with pressure modulation do you --

DR. VANIER:

You mean the spin exchange shift itself?

MR. HOWE:

Yes.

DR. VANIER:

Well, I think that we have shown that in the past a long time ago and of course there are small effects, second order effects, but

we have shown that the spin exchange tuning technique, the broadening technique used cancels exactly within the first order the spin exchange shift.

The cavity is mistuned by this process in such a way that the spin exchange shift is canceled, which you don't have in other types of tuning. Yes, that is the whole secret; I think that we have shown that a long time ago, to a great accuracy.

MR. HOWE:

My problem is being able to separate out the --

DR. VANIER:

In the passive time.

MR. HOWE:

Yes.

DR. VANIER:

Oh, in the passive time then you don't use spin exchange broadening to change the maser, in that case you use spin exchange exactly -- you can prove mathematically and it works out in practice that once you have found that point where your frequency is independent of pressure it is a simple point.

DR. REINHARDT, NASA/Goddard

Are you setting up any devices to measure magnetic shift and anomalous spin exchange shifts, because they can be on the order of several parts in 10^{13}.

DR. VANIER:

You are talking about ε_M or ε_H?

DR. REINHARDT:

Yes.

DR. VANIER:

No, not yet. I am not there yet.

DR. REINHARDT:

But, are you going to?

DR. VANIER:

Yes, we think that we will be able to do that, yes.

DR. REINHARDT:

Okay.

DR. VANIER:

But, I will talk to you about it.